SIAM J. APPL. MATH.
Vol. 76, No. 4, pp. 1737–1763

STEKLOFF EIGENVALUES IN INVERSE SCATTERING*

F. CAKONI†, D. COLTON‡, S. MENG‡, AND P. MONK§

Abstract. We consider a problem in nondestructive testing in which small changes in the (possibly complex valued) refractive index $n(x)$ of an inhomogeneous medium of compact support are to be determined from changes in measured far field data due to incident plane waves. The problem is studied by considering a modified far field operator $\mathcal{F}$ whose kernel is the difference of the measured far field pattern due to the scattering object and the far field pattern of an auxiliary scattering problem with the Stekloff boundary condition imposed on the boundary of a domain B, where B is either the support of the scattering object or a ball containing the scattering object in its interior. It is shown that $\mathcal{F}$ can be used to determine the Stekloff eigenvalues corresponding to B, where, if $B \neq D$, the refractive index is set equal to one in $B \setminus \overline{D}$. A formula is obtained relating changes in $n(x)$ to changes in the Stekloff eigenvalues and numerical examples are given showing the effectiveness of determining changes to the refractive index in this way.

Key words. inverse scattering, nondestructive testing, Stekloff eigenvalues, Herglotz wave functions

AMS subject classifications. 35R30, 35J25, 35P25, 35P05

DOI. 10.1137/16M1058704

1. Introduction.

In recent years there has been considerable interest in transmission eigenvalues and their application. For a glimpse at the many different directions that this research has taken we refer the reader to the special issue of *Inverse Problems* edited by F. Cakoni and H. Haddar [7]. Of particular interest to us is the potential use of transmission eigenvalues in nondestructive testing [6, 8]. In particular, transmission eigenvalues can be determined from the measured scattering data and carry information about the refractive index of nonabsorbing media [9].

However the use of transmission eigenvalues in nondestructive testing has two major drawbacks. The first drawback is that in general only the first transmission eigenvalue can be accurately determined from the measured data [4] and the determination of this eigenvalue means that the frequency of the interrogating wave must be varied in a frequency range around this eigenvalue. In particular, multifrequency data must be used in an a priori determined frequency range. This also requires the medium to be nondispersive. The second drawback is that only real transmission eigenvalues can be conveniently determined from the measured scattering data which means that transmission eigenvalues cannot be used for the nondestructive testing of inhomogeneous absorbing media. The purpose of this paper is to overcome these difficulties by using Stekloff eigenvalues instead of transmission eigenvalues.

The plan of our paper is as follows. In the remainder of this section we will introduce the scattering problem for an inhomogeneous medium that we will be considering

*Received by the editors January 27, 2016; accepted for publication (in revised form) May 25, 2016; published electronically August 30, 2016.
http://www.siam.org/journals/siap/76-4/M105870.html
Funding: This research was supported in part by AFOSR grant FA9550-13-1-0199 and NSF grant DMS1602802.
†Department of Mathematics, Rutgers University, Piscataway, NJ 08854-8019 (fc292@math.rutgers.edu).
‡Department of Mathematical Sciences, University of Delaware, Newark, DE 19716 (colton@udel.edu, sxmeng@udel.edu).
§Corresponding author. Department of Mathematical Sciences, University of Delaware, Newark, DE 19716 (monk@udel.edu).

and establish a connection between a modified far field operator and the Stekloff eigenvalues associated with this inhomogeneous medium. Next, restricting our attention to the simple case when the refractive index is real valued, in section 2 we establish the existence of Stekloff eigenvalues in this case and derive a relationship between small changes in the refractive index and the corresponding change in the Stekloff eigenvalue. We then proceed in section 3 to make this connection more precise and show how Stekloff eigenvalues can be determined from a far field equation associated with this modified far field operator. This is followed in section 4 by consideration of the non-self-adjoint Stekloff eigenvalue problem for a complex valued refractive index using Agmon's theory of non-self-adjoint eigenvalue problems [2]. Our paper is concluded by providing a variety of numerical examples, mostly for the special case of nonabsorbing media, showing the efficiency of our approach to determining qualitative estimates of changes in the refractive index from measurements of the far field data.

Although we have assumed throughout this paper that our measured data are far field data, all of our results can be modified in a straightforward manner to the case when near field data are used.

Suppose D is a bounded domain in $\mathbb{R}^m$, $m = 2, 3$, with boundary ∂D of class C^2 and that the origin lies in D. The forward scattering problem we shall consider is to find $u \in C^2(\mathbb{R}^m \setminus \overline{D}) \cap C^1(\mathbb{R}^m \setminus D)$ such that

$$\begin{aligned} \Delta u + k^2 n(x) u &= 0 \text{ in } \mathbb{R}^m, \\ u(x) &= \exp(ikx \cdot d) + u^s(x), \\ \lim_{r\to\infty} r^{\frac{m-1}{2}} \left(\frac{\partial u^s}{\partial r} - iku^s \right) &= 0 \text{ uniformly with respect to } \hat{x} := x/|x|, \end{aligned} \tag{1.1}$$

where $r = |x|$, the refractive index $n \in L^\infty(\mathbb{R}^m)$ satisfies $\Re(n(x)) > 0$, $\Im(n(x)) \geq 0$, and $n(x) = 1$ for $x \in \mathbb{R}^m \setminus \overline{D}$. Then the far field pattern u_∞ of the scattered field u^s is defined by

$$u^s(x) = \frac{\exp(ikr)}{r^{\frac{m-1}{2}}} u_\infty(\hat{x}, d) + O\left(\frac{1}{r^{\frac{m+1}{2}}} \right), \ r \to \infty,$$

where $\hat{x} = x/|x|$ (cf. [9]).

Now let B either be a ball centered at the origin containing D in its interior or $B = D$ and let $h \in C^2(\mathbb{R}^m \setminus \overline{B}) \cap C^1(\mathbb{R}^m \setminus B)$ be such that

$$\begin{aligned} \Delta h + k^2 h &= 0 \text{ in } \mathbb{R}^m \setminus \overline{B}, \\ h(x) &= \exp(ikx \cdot d) + h^s(x), \\ \frac{\partial h}{\partial \nu} + \lambda h &= 0 \text{ on } \partial B, \\ \lim_{r\to\infty} r^{\frac{m-1}{2}} \left(\frac{\partial h^s}{\partial r} - ikh^s \right) &= 0 \text{ uniformly with respect to } \hat{x}, \end{aligned} \tag{1.2}$$

where ν is the unit outward normal to B and λ is a constant such that $\Im(\lambda) \geq 0$. Let

$$h^s(x) = \frac{\exp(ikr)}{r^{\frac{m-1}{2}}} h_\infty(\hat{x}, d) + O\left(\frac{1}{r^{\frac{m+1}{2}}} \right), \ r \to \infty.$$

Note that there exists a unique solution to (1.2) since if h_1 and h_2 were two solutions then $h = h_1 - h_2$ satisfies the radiation condition and

$$\Im \int_{\partial B} h \frac{\partial \overline{h}}{\partial \nu} \, ds = \Im(\lambda) \int_{\partial B} |h|^2 \, ds = 0.$$

Thus uniqueness holds by [9, Theorem 2.13] and then existence follows by the straightforward use of potential theory (cf. [9, Theorem 3.12] for the Neumann problem).

We now give a heuristic argument linking a modified far field equation with Stekloff eigenvalues. Suppose $g \in L^2(S)$ is a nontrivial solution of

$$\int_S [u_\infty(\hat{x}, d) - h_\infty(\hat{x}, d)] g(d)\, ds(d) = 0, \tag{1.3}$$

where $S := \{x : |x| = 1\}$. If we define the Herglotz wave function by

$$v_g(x) := \int_S \exp(ikx \cdot d)\, g(d)\, ds(d), \tag{1.4}$$

then

$$w_\infty(\hat{x}) := \int_S u_\infty(\hat{x}, d)\, g(d)\, ds(d)$$

is the far field pattern for

$$\begin{aligned} \Delta w + k^2 n(x) w &= 0 \text{ in } \mathbb{R}^m, \\ w(x) &= v_g(x) + w^s(x), \\ \lim_{r\to\infty} r^{\frac{m-1}{2}} \left(\frac{\partial w^s}{\partial r} - ikw^s \right) &= 0 \text{ uniformly with respect to } \hat{x}, \end{aligned} \tag{1.5}$$

and

$$v_\infty(\hat{x}) := \int_S h_\infty(\hat{x}, d)\, g(d)\, ds(d)$$

is the far field pattern for

$$\begin{aligned} \Delta v + k^2 v &= 0 \text{ in } \mathbb{R}^m \setminus \overline{B}, \\ v(x) &= v_g(x) + v^s(x), \\ \frac{\partial v}{\partial \nu} + \lambda v &= 0 \text{ on } \partial B, \\ \lim_{r\to\infty} r^{\frac{m-1}{2}} \left(\frac{\partial v^s}{\partial r} - ikv^s \right) &= 0 \text{ uniformly with respect to } \hat{x}. \end{aligned} \tag{1.6}$$

From (1.3) we have that $w_\infty(\hat{x}) = v_\infty(\hat{x})$, i.e., by Rellich's lemma $w(x) = v(x)$ in $\mathbb{R}^m \setminus D$, where we have used the fact that if B is a ball the solution of (1.2) can be extended as a solution of $\Delta h + k^2 h = 0$ in $\mathbb{R}^m \setminus \{0\}$. In particular, since $w(x)$ is a solution of the Helmholtz equation in $\mathbb{R}^m \setminus \overline{D}$ it is necessary that $v(x)$ also has this property.

Hence w satisfies the boundary value problem

$$\begin{aligned} \Delta w + k^2 n(x) w &= 0 \text{ in } B, \\ \frac{\partial w}{\partial \nu} + \lambda w &= 0 \text{ on } \partial B. \end{aligned} \tag{1.7}$$

The solution of (1.7) will be identically zero unless λ is a *Stekloff eigenvalue*. In this case there exists a nontrivial solution of (1.3), i.e., we can determine the Stekloff eigenvalues of (1.7) and hence detect changes in $n(x)$. In the following sections we place the above heuristic arguments on a rigorous basis. We end this section with a more formal definition of the Stekloff eigenvalue.

DEFINITION 1.1. *For fixed k, $\lambda := \lambda(k) \in \mathbb{C}$ is called a Stekloff eigenvalue if the homogeneous problem* (1.7) *has a nontrivial solution $u \in H^1(B)$.*

2. The Stekloff eigenvalue problem for real $n(x)$. We now want to pose the Stekloff eigenvalue problem variationally. From (1.7), we have that $w \in H^1(B)$ and λ satisfy

$$(\nabla w, \nabla \xi) - k^2(nw, \xi) = -\lambda \langle w, \xi \rangle \quad \forall \xi \in H^1(B), \tag{2.1}$$

where

$$(f, g) = \int_B f\, \overline{g}\, dA \text{ and } \langle f, g \rangle = \int_{\partial B} f\, \overline{g}\, ds.$$

Provided k^2 is not an interior Neumann eigenvalue for the Laplacian on B we can define the Neumann-to-Dirichlet map $T : L^2(\partial B) \to L^2(\partial B)$ as follows. Let $\mu \in L^2(\partial D)$ and define $v_\mu \in H^1(B)$ to be the solution of

$$(\nabla v_\mu, \nabla \xi) - k^2(nv_\mu, \xi) = \langle \mu, \xi \rangle \quad \forall \xi \in H^1(B). \tag{2.2}$$

Then

$$T\mu = v_\mu|_{\partial B}. \tag{2.3}$$

Thus $\mu \in L^2(\partial B)$ is a Stekloff eigenfunction with eigenvalue λ if and only if it is a nontrivial solution of

$$-\lambda T\mu = \mu. \tag{2.4}$$

Of course, since $T\mu \in H^{1/2}(\partial B)$ and $H^{1/2}(\partial B)$ is compactly embedded in $L^2(\partial B)$, we can see that T is compact.

If n is real, then T is also self-adjoint. To see this it suffices to consider real functions $\xi, \mu \in L^2(\partial B)$. Then

$$\langle T\xi, \mu \rangle = \langle v_\xi, \mu \rangle = (\nabla v_\xi, \nabla v_\mu) - k^2(nv_\xi, v_\mu) = \langle \xi, v_\mu \rangle = \langle \xi, T\mu \rangle.$$

So in this case Stekloff eigenvalues exist, are real, and are discrete. The existence of Stekloff eigenvalues when n is complex will be proved in section 4.

Now suppose n is perturbed by δn giving rise to a change in eigenfunction $w \in H^1(B)$ by δw and eigenvalue by $\delta\lambda$. Then $\delta w \in H^1(B)$ and $\delta\lambda$ satisfy

$$\begin{aligned}(\nabla(w + \delta w), \nabla \xi) - k^2((n + \delta n)(w + \delta w), \xi) \\ = -(\lambda + \delta\lambda)\langle (w + \delta w), \xi \rangle \quad \forall \xi \in H^1(B).\end{aligned}$$

Using the fact that (w, λ) are a real eigenpair we have that

$$\begin{aligned}(\nabla \delta w, \nabla \xi) - k^2(\delta n(w + \delta w), \xi) - k^2(n\delta w, \xi) \\ = -\delta\lambda\langle (w + \delta w), \xi \rangle - \lambda\langle \delta w, \xi \rangle \quad \forall \xi \in H^1(B).\end{aligned}$$

Choosing $\xi = w$ to be an eigenfunction, and using the fact that n is assumed to be real, we have that

$$k^2(\delta n(w + \delta w), w) = \delta\lambda\langle (w + \delta w), w \rangle.$$

Assuming only small changes we have (neglecting quadratic terms!) that

$$\delta\lambda \approx \frac{k^2(\delta nw, w)}{\langle w, w \rangle}. \tag{2.5}$$

Close to a Dirichlet eigenvalue it could occur that $w \approx 0$ on ∂B in which case it may be that the method becomes very sensitive to changes in n. Note that in general there is no upper bound for the maximum Stekloff eigenvalue that is independent of k.

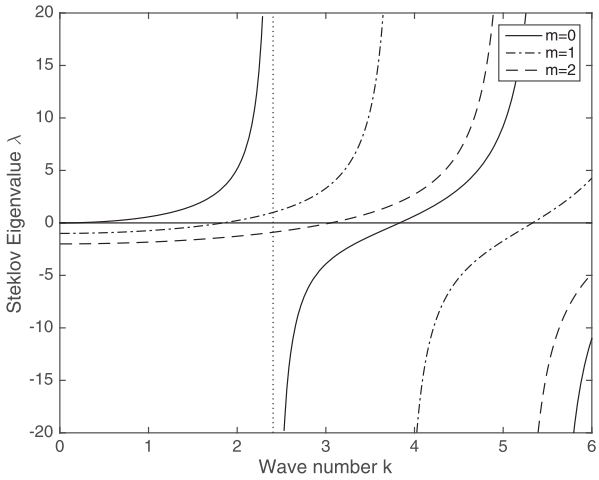

FIG. 1. *Stekloff eigenvalues for the unit disk in* $\mathbb{R}^2$ *with* $n(x) = 1$ *given by* (2.6) *for different choices of* m *as functions of wave number* k*. For small* k *the eigenvalues are bounded above. At the first Dirichlet eigenvalue (in this case* $k \approx 2.404825558$ *marked by a dotted line in the graph) the branch of eigenvalues corresponding to* $m = 0$ *has a vertical asymptote and so there is no upper or lower bound that is* k *independent.*

Example 1. We now consider an example in $\mathbb{R}^2$ to illustrate some of the previous comments. In particular, for a disk of radius 1 in $\mathbb{R}^2$ with $n(x) = n$ constant, the mth Stekloff eigenvalue is

$$\lambda_m = -k\sqrt{n}\frac{J_m'(k\sqrt{n})}{J_m(k\sqrt{n})}, \quad m = 0, 1, 2, \ldots, \tag{2.6}$$

where J_m denotes the Bessel function of order m.

We choose $n = 1$. As k approaches a Dirichlet eigenvalue, one of the λ_m has a vertical asymptote and changes sign across the Dirichlet eigenvalue (see Figure 1). Note that for fixed k there is in general no possible lower bound although there does exist an upper bound for λ_m provided k is not a Dirichlet eigenvalue (from the asymptotics of the Bessel function for large m there is no lower bound because $\lambda_m \to -\infty$ as $m \to \infty$, at least for the disk).

We can derive the following upper bound for the Stekloff eigenvalue λ if k is small enough. If w is the eigenfunction corresponding to the eigenvalue λ then

$$\lambda = \frac{k^2(nw, w) - (\nabla w, \nabla w)}{\langle w, w\rangle} \leq \frac{k^2 n_{\max}(w, w) - (\nabla w, \nabla w)}{\langle w, w\rangle},$$

where $n_{\max} = \max_B(n)$. But the Poincaré inequality states that

$$(w, w) \leq C_p[(\nabla w, \nabla w) + \langle w, w\rangle],$$

where C_p is a constant independent of w. So

$$\lambda \leq (C_p n_{\max} k^2 - 1)\frac{(\nabla w, \nabla w)}{\langle w, w\rangle} + k^2 n_{\max} C_p,$$

and if $k^2 \leq 1/(C_p n_{\max})$ we have

$$\lambda \leq k^2 n_{\max} C_p. \tag{2.7}$$

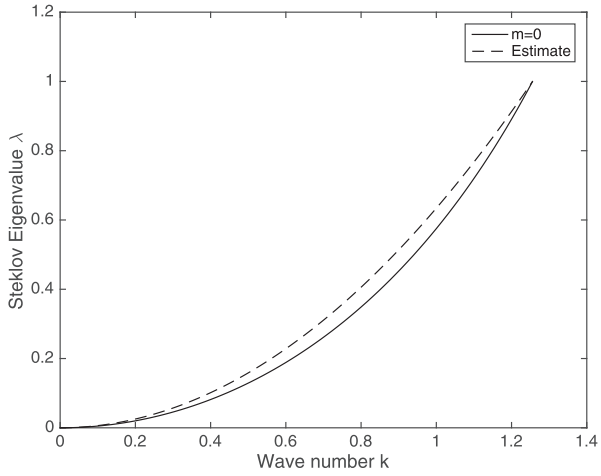

FIG. 2. *The Stekloff eigenvalue for the unit disk in* $\mathbb{R}^2$ *with* $n(x) = 1$ *given by* (2.6) *for* $m = 0$ *and the upper bound* (2.7) *as a function of* k *for* $0 \le k \le 1/C_p$ *(here* $n_{\max} = 1$*). The interval where the bound holds is sharp in this case.*

In particular $C_p = 1/\chi^2$, where χ^2 is the first eigenvalue and $z \in H^1(B)$, $z \neq 0$, is the corresponding eigenfunction satisfying

$$(\nabla z, \nabla v) = \chi^2(z, v) - \langle z, v\rangle \qquad \text{for all } v \in H^1(B).$$

Example 2. For a disk of radius 1 in $\mathbb{R}^2$ the eigenvalues of the above equation are the roots of the transcendental equations $\chi J_m'(\chi) + J_m(\chi) = 0$, $\quad m = 0, 1, \ldots$. When $m = 0$ we compute the numerical approximation to the first eigenvalue $\chi_0 \approx 1.256\ldots$ and hence $C_p \approx 0.6341\ldots$. In Figure 2 we show a graph of the Stekloff eigenvalues for a disk with radius 1 in $\mathbb{R}^2$ and $n = 1$, together with the upper bound given by our estimate (2.7). Clearly, for the special case of this disk, our estimate and its range of validity are reasonable.

Next we consider the special case of a small perturbation of the background in the unit disk in $\mathbb{R}^2$, where $n(x)$ is given by $(1+n_1)^2$ in the disk of radius $a < 1$ centered at the origin and $n(x) = 1$ for $a < |x| < 1$. Considering the lowest order eigenfunction, we need to compute the general radially symmetric solution of the Helmholtz equation

$$\Delta u + k^2(1 + \chi_{B_a(0)} n_1)^2 u = 0 \text{ in } B_1(0),$$

where $\chi_{B_a(0)}$ is the indicator function for the disk in $\mathbb{R}^2$ of radius a centered at the origin. The solution is given by

$$u = A \begin{cases} J_0(kn_1 r), & 0 \le r < a, \\ c_1 J_0(kr) + c_2 Y_0(kr), & a < r \le 1, \end{cases}$$

where A is an arbitrary constant and, for small ka,

$$c_1 = 1 - \frac{1}{4}k^2 n_1(n_1+2)(2\ln(2) - 2\ln(ka) - 2\gamma + 1)a^2 + O\left((ka)^4\right),$$
$$c_2 = -\frac{1}{4}k^2 n_1(2+n_1)\pi a^2 + O\left((ka)^4\right),$$

where γ is Euler's constant. Using the above solution in the Stekloff boundary con-

dition we obtain, for small ka,

$$\lambda = \lambda_0 + \frac{1}{2} n_1 (2 + n_1)(ka)^2 + O((ka)^4),$$

where λ_0 is the eigenvalue corresponding to $a = 0$. Hence the perturbation in the eigenvalue is proportional to n_1 and the area of the perturbation (i.e., proportional to a^2) for small a and n_1, as is to be expected from our previous perturbation result (2.5).

Although, in the above analysis we have assumed that n is real valued, the formulation of the eigenvalue problem remains the same for complex valued n. In particular, the formulas (2.5) and (2.6) are still valid for complex valued n. However, if n is complex the Stekloff eigenvalue problem is no longer self-adjoint and this case will be examined in section 4.

3. Determination of eigenvalues from far field data. We now want to show that Stekloff eigenvalues can be determined from far field data. Throughout this section we allow for the possibility that $n(x)$ may be complex valued. To this end, we first discuss some auxiliary results. Let $f \in H^{-1/2}(\partial B)$ and consider the problem of finding $w \in H^1(B)$ such that

$$\begin{aligned} \Delta w + k^2 n(x) w &= 0 \text{ in } B, \\ \frac{\partial w}{\partial \nu} + \lambda w &= f \text{ on } \partial B. \end{aligned} \tag{3.1}$$

Recalling Definition 1.1 we have the following result.

LEMMA 3.1. *Assume that λ is not a Stekloff eigenvalue. Then* (3.1) *has a unique solution $u \in H^1(B)$. This solution can be decomposed as $u = u^i + u^s$, where $u^i \in H^1(B)$ solves the Helmholtz equation in B and $u^s \in H^1_{loc}(\mathbb{R}^m)$ is a radiating field (i.e., satisfies the Sommerfeld radiation condition).*

Proof. Solvability of (3.1) when λ is not a Stekloff eigenvalue is well known [9]. For later use, we briefly present here an equivalent variational formulation of (3.1) which reads find $u \in H^1(B)$ such that

$$\int_B (\nabla u \nabla \overline{\varphi} - k^2 n u \overline{\varphi})\, dx + \lambda \int_{\partial B} u\, \overline{\varphi}\, ds = \int_{\partial B} f\, \overline{\varphi}\, ds \qquad \text{for all } \varphi \in H^1(B). \tag{3.2}$$

This leads to a Fredholm equation,

$$\mathbb{A}u + \mathbb{B}u = \ell,$$

to solve where the coercive bounded linear operator $\mathbb{A} : H^1(B) \to H^1(B)$ is defined by

$$(\mathbb{A}u, \varphi)_{H^1(B)} := \int_B (\nabla u \nabla \overline{\varphi} + u\, \overline{\varphi})\, dx,$$

the compact bounded linear operator $\mathbb{B} : H^1(B) \to H^1(B)$ is defined by

$$(\mathbb{B}u, \varphi)_{H^1(B)} := -\int_B ((1 + k^2 n) u\, \overline{\varphi})\, dx + \lambda \int_{\partial B} u\, \overline{\varphi}\, ds,$$

and $\ell \in H^1(B)$ is defined by

$$(\ell, \varphi)_{H^1(B)} := \int_{\partial B} f\, \overline{\varphi}\, ds. \tag{3.3}$$

Let us recall that the radiating fundamental solution $\Phi(\cdot,\cdot)$ of the Helmholtz equation in $\mathbb{R}^m$ is defined by

$$\Phi(x,z) := \begin{cases} \dfrac{e^{ik|x-z|}}{4\pi|x-z|} & \text{in } \mathbb{R}^3, \\ \dfrac{i}{4}H_0^{(1)}(k|x-z|) & \text{in } \mathbb{R}^2, \end{cases} \tag{3.4}$$

where $H_0^{(1)}$ denotes a Hankel function of the first kind of order zero. Then Green's representation formula applied to the solution $u \in H^1(B)$ gives

$$u(x) = \int_{\partial B} \left(\frac{\partial u(y)}{\partial \nu}\Phi(x,y) - \frac{\partial \Phi(x,y)}{\partial \nu}u(y) \right) ds_y - k^2 \int_B \Phi(x,y)(1-n(y))u(y)\,dy$$

and this provides the desired decomposition, where

$$u^i(x) := \int_{\partial B} \left(\frac{\partial u(y)}{\partial \nu}\Phi(x,y) - \frac{\partial \Phi(x,y)}{\partial \nu}u(y) \right) ds_y, \qquad x \in B, \tag{3.5}$$

satisfies the Helmholtz equation in B and

$$u^s(x) := -k^2 \int_B \Phi(x,y)(1-n(y))u\,dy, \qquad x \in \mathbb{R}^m,$$

satisfies the Sommerfeld radiation condition. ∎

Define $\mathcal{F} : L^2(S) \to L^2(S)$ by

$$(\mathcal{F}g)(\hat{x}) = \int_S [u_\infty(\hat{x},d) - h_\infty(\hat{x},d)]\, g(d)\, ds(d).$$

Then $\mathcal{F}$ is injective unless λ is a Stekloff eigenvalue with eigenfunction of the form $w(x) = v_g(x) + w^s(x)$ (cf. our discussion in the introduction to this paper and [9, Theorem 10.9]). Since u_∞ and h_∞ satisfy the reciprocity relation $\mathcal{F}$ is injective with dense range if and only if there does not exist a Stekloff eigenfunction for B which has the above decomposition (cf. [9, Theorem 3.22]). We will show that Stekloff eigenvalues can now be obtained by solving in an appropriate way the following modified far field equation: find $g \in L^2(S)$ such that

$$\mathcal{F}g = \Phi_\infty(\hat{x}, z), \tag{3.6}$$

where $\Phi_\infty(\hat{x}, z)$ is the far field pattern of the fundamental solution (3.4). Unfortunately, in general the above modified far field equation cannot be solved for any $z \in B$. Indeed, if $g_z \in L^2(S)$ satisfies (3.6) then by Rellich's lemma

$$w_z^s(x) - v_z^s(x) = \Phi(x,z) \qquad \text{for } x \in \mathbb{R}^m \setminus \overline{B},$$

where w_z^s and v_z^s are defined by (1.5) and (1.6), respectively, with $v_g := v_{g_z}$. Thus, w_z must solve the problem

$$\begin{aligned} &\Delta w_z + k^2 n(x) w_z = 0 \text{ in } B, \\ &\frac{\partial w_z}{\partial \nu} + \lambda w_z = \frac{\partial \Phi(\cdot,z)}{\partial \nu} + \lambda \Phi(\cdot,z) \text{ on } \partial B \end{aligned} \tag{3.7}$$

with the additional property that

$$w_z = v_{g_z} + w_z^s \qquad \text{in } \mathbb{R}^m. \tag{3.8}$$

Unfortunately, the unique solution of (3.7) (provided that λ is not a Stekloff eigenvalue for fixed k^2) in general does not assume a decomposition of the form (3.8) with v_{g_z} being a Herglotz wave function. However according to Lemma 3.1 w_z can be decomposed as $w_z(x) = w_z^i(x) + w_z^s(x)$ for $x \in B$, where $w_z^i \in H^1(B)$ satisfies the Helmholtz equation in B and $w_z^s \in H^2_{loc}(\mathbb{R}^m)$ is a radiating solution to

$$\begin{aligned} \Delta w_z^s + k^2 n(x) w_z^s &= k^2(1-n(x))w_z^i \qquad \text{in } \mathbb{R}^m, \\ \lim_{r\to\infty} r^{\frac{m-1}{2}} \left(\frac{\partial w_z^s}{\partial r} - ikw_z^s \right) &= 0 \text{ uniformly with respect to } \hat{x}. \end{aligned} \tag{3.9}$$

Note that $1-n$ is supported inside B, more precisely, in $\overline{D}$. Hence the kernel g of the Herglotz function v_g that approximates the above w_z^i in the $H^1(B)$ norm (cf. [9, Theorem 5.21]) satisfies

$$\|\mathcal{F}g - \Phi_\infty(\cdot, z)\|_{L^2(S)} < \epsilon.$$

Let us define the space of generalized incident waves

$$H_{inc}(B) := \left\{ v^i \in H^1(B) : \ \Delta v^i + k^2 v^i = 0 \right\}.$$

We have that the operator $\mathcal{F} : L^2(S) \to L^2(S)$ can be factored as $\mathcal{F}g = \mathcal{B}v_g$, where $\mathcal{B} : H_{inc}(B) \to L^2(S)$ is defined as

$$\mathcal{B} = G_w P_D - G_v$$

with $G_v : H_{inc}(B) \to L^2(S)$ mapping $v^i \mapsto v_\infty$, where v_∞ is the far field pattern of v^s that solves

$$\begin{aligned} \Delta v^s + k^2 v^s &= 0 \text{ in } \mathbb{R}^m \setminus \overline{B}, \\ \frac{\partial v^s}{\partial \nu} + \lambda v^s &= -\frac{\partial v^i}{\partial \nu} - \lambda v^i \text{ on } \partial B, \\ \lim_{r\to\infty} r^{\frac{m-1}{2}} \left(\frac{\partial v^s}{\partial r} - ikv^s \right) &= 0 \text{ uniformly with respect to } \hat{x}, \end{aligned} \tag{3.10}$$

$P_D : H_{inc}(B) \to L^2(D)$ mapping v^i to $k^2(1-n)v^i$, and $G_w : L^2(D) \to L^2(S)$ mapping $f \mapsto w_\infty$, where w_∞ is the far field pattern of w^s that solves

$$\begin{aligned} \Delta w_z^s + k^2 n w_z^s &= f \qquad \text{in } \mathbb{R}^m, \\ \lim_{r\to\infty} r^{\frac{m-1}{2}} \left(\frac{\partial w_z^s}{\partial r} - ikw_z^s \right) &= 0 \text{ uniformly with respect to } \hat{x}, \end{aligned} \tag{3.11}$$

($f = 0$ outside D). Note that the solution operators G_v and G_w are bounded and compact whereas P_D is bounded. By construction we have that

$$\mathcal{B}v^i = \Phi_\infty(\cdot, z), \qquad z \in D,$$

has a solution $v^i := w_z^i$, where w_z^i is defined by (3.7) and (3.9).

The following two theorems provide a method to compute Stekloff eigenvalues from far field measured scattering data at a given fixed frequency k (compare to [5] for transmission eigenvalues). The above discussion is a proof of the following theorem.

THEOREM 3.2. *Assume that λ is a not Stekloff eigenvalue and let $z \in D$. Then, for every $\epsilon > 0$ there exists a $g_\epsilon^z \in L^2(S)$ that satisfies*

$$\lim_{\epsilon \to 0} \|\mathcal{F} g_\epsilon^z - \Phi_\infty(\cdot, z)\|_{L^2(S)} = 0 \tag{3.12}$$

such that $\lim_{\epsilon\to 0} \|v_{g_\epsilon^z} - w_z^i\|_{H^1(B)} = 0$ and hence $\|v_{g_\epsilon^z}\|_{H^1(B)}$ is bounded as $\epsilon \to 0$, where $v_{g_\epsilon^z}$ is the Herglotz wave function with kernel g_ϵ^z.

Now we show that if λ is a Stekloff eigenvalue, then all $g_\epsilon^z \in L^2(S)$ that satisfy (3.12) are such that $\|v_{g_\epsilon^z}\|_{H^1(D)}$ blows up as $\epsilon \to 0$. Note that if λ is a Stekloff eigenvalue, (3.12) will be satisfied provided $\mathcal{F}$ has dense range. This in turn will be satisfied provided $\mathcal{F}$ is injective (cf. the proof of [9, Theorem 3.22]), i.e., the u^i in Lemma 3.1 is not a Herglotz wave function (cf. [6]).

THEOREM 3.3. *Assume that λ is a Stekloff eigenvalue and $g_\epsilon^z \in L^2(S)$ satisfies (3.12). Then $\|v_{g_\epsilon^z}\|_{H^1(B)}$ cannot be bounded as $\epsilon \to 0$ for almost every $z \in B_\rho$, where $B_\rho \subset D$ is an arbitrary ball of radius ρ.*

Proof. Assume to the contrary that for $z \in B_\rho \subset D$, where B_ρ is a small ball of radius ρ, $\|v_{g_\epsilon^z}\|_{H^1(B)}$ is bounded as $\epsilon \to 0$, i.e., up to a subsequence the $v_{g_\epsilon^z}$ converge weakly to a $v^i \in H_{inc}(B)$. By compactness of $\mathcal{B}$ we conclude that

$$\lim_{\epsilon \to 0} \|\mathcal{B} v_{g_\epsilon^z} - \mathcal{B} v^i\|_{L^2(S)} = \lim_{\epsilon \to 0} \|\mathcal{F} g_\epsilon^z - \mathcal{B} v^i\|_{L^2(S)} = 0.$$

Hence $\mathcal{B} v^i = \Phi_\infty(\cdot, z)$ and from Rellich's lemma and the definition of $\mathcal{B}$ we see in the same way as in the above discussion that $w := w^s + v^i$, where w^s satisfies (3.9) with w_z^i replaced by v^i satisfies (3.7). But from Lemma 3.1, (3.7) is solvable if and only if ℓ defined by (3.3) is orthogonal to each w_λ in the kernel of the adjoint operator $\mathbb{A}^* + \mathbb{B}^*$, i.e., to $w_\lambda \in H^1(D)$ satisfying

$$\begin{aligned} \Delta w_\lambda + k^2 \overline{n} w_\lambda &= 0 \text{ in } B, \\ \frac{\partial w}{\partial \nu} + \overline{\lambda} w_\lambda &= 0 \text{ on } \partial B. \end{aligned}$$

Thus

$$\int_{\partial B} \left(\frac{\partial \Phi(\cdot, z)}{\partial \nu} + \lambda \Phi(\cdot, z) \right) \overline{w_\lambda}\, ds = 0,$$

which from the boundary condition satisfied by $\overline{w_\lambda}$ on ∂B becomes

$$\int_{\partial B} \left(\frac{\partial \Phi(\cdot, z)}{\partial \nu} \overline{w_\lambda} - \Phi(\cdot, z) \frac{\partial \overline{w_\lambda}}{\partial \nu} \right) ds = 0.$$

Green's representation implies that $w_\lambda(z) = 0$ for z in a subset of B with nonzero measure. The unique continuation principle [9] now implies that $w_\lambda \equiv 0$ in B which is a contradiction. ∎

4. The Stekloff eigenvalue problem for complex $n(x)$. In the interesting case of absorbing media, i.e., for complex valued refractive index $n(x) = n_1(x) + i\frac{n_2(x)}{k}$, $n_1(x) > 0$ and $n_2(x) \geq 0$ (and n_2 not identically zero) for $x \in B$, the Stekloff eigenvalue problem is a non-self-adjoint eigenvalue problem. Hence the existence of its eigenvalues is now a more complicated matter. Obviously, the operator T defined in (2.4) is still compact (but non-self-adjoint) for complex n, and hence we know that the Stekloff eigenvalue problem satisfies all the spectral properties of a compact

operator, in particular, the Stekloff eigenvalues form at most a discrete set without an accumulation point in $\mathbb{C}$. In fact, for complex n there are no real Stekloff eigenvalues, which can be seen by taking $\varphi = u$ and $f = 0$ in (3.2) to obtain

$$\int_B \left(|\nabla u|^2 - k^2 n|u|^2\right)\, dx + \lambda \int_{\partial B} |u|^2\, ds = 0.$$

Taking the imaginary part of this equality,

$$\Im(\lambda) \int_{\partial B} |u|^2\, ds = k^2 \int_B \Im(n)|u|^2\, dx. \tag{4.1}$$

Noting that, since $n_2 \neq 0$, k^2 cannot be a Dirichlet eigenvalue of the Laplacian on B, we conclude $\Im(\lambda) > 0$.

The goal of this section is to show that there are indeed infinitely many complex eigenvalues and to give an indication of where they are in the complex plane. Our approach to the analysis of Stekloff spectral properties follows [13] and is based on the spectral theory of non-self-adjoint operators by Agmon [2]. Since our approach uses pseudodifferential calculus, in this section we must assume that the boundary ∂B is of class C^∞, and $n \in C^\infty(\overline{B})$.

For a fixed z, we introduce an operator B_z defined on $H^{\frac{1}{2}}(\partial B)$ by

$$B_z : \alpha \mapsto g, \tag{4.2}$$

where

$$g = \frac{\partial u}{\partial \nu} - zu \tag{4.3}$$

and $u \in H^1(D)$ satisfies the Dirichlet problem

$$\Delta u + k^2 n u = 0 \quad \text{in} \quad B, \tag{4.4}$$

$$u = \alpha \quad \text{on} \quad \partial B. \tag{4.5}$$

Clearly B_z continuously maps $H^{\frac{1}{2}}(\partial B)$ to $H^{-\frac{1}{2}}(\partial B)$, since the fact that n is not real valued implies that a unique solution to (4.4)–(4.5) exists.

One observes that $-\lambda$ is a Stekloff eigenvalue if and only if $\lambda - z$ is an eigenvalue of B_z. The analysis of Stekloff eigenvalues will then be obtained from the analysis of the spectrum of the operator B_z or more precisely of its inverse R_z that will be shown to exist for a well-chosen parameter z. To show the latter we need to prove certain regularity results formulated in the following technical lemma where, roughly speaking, we show that α is bounded by g in appropriate norms for a set of appropriately chosen $z \in \mathbb{C}$.

LEMMA 4.1. *Assume* $\arg z$ *is fixed and* $\arg z \neq 0$. *Let* α *and* g *be defined by* (4.2) *for* $\alpha \in H^{\frac{1}{2}}(\partial B)$ *and* $g \in H^{-\frac{1}{2}}(\partial B)$. *Moreover assume that* $g \in H^{s-\frac{1}{2}}(\partial B)$ *for* $s \geq 0$. *Then for sufficiently large* $|z|$

$$\|\alpha\|_{H^{s-\frac{1}{2}}(\partial B)} \leq C \frac{1}{|z|} \|g\|_{H^{s-\frac{1}{2}}(\partial B)} \qquad \textit{and}$$

$$\|\alpha\|_{H^{s+\frac{1}{2}}(\partial B)} \leq C \|g\|_{H^{s-\frac{1}{2}}(\partial B)}$$

for some positive constant $C > 0$.

Proof. Let $u \in H^1(B)$ satisfy (4.4), (4.5). Then $B_z\alpha = g$ implies

$$\begin{aligned} \Delta u + k^2 n u &= 0 \quad \text{in} \quad B, \\ \frac{\partial u}{\partial \nu} - zu &= g \quad \text{on} \quad \partial B. \end{aligned}$$

Classical regularity results for boundary value problems for elliptic operators (see, e.g., [15]) imply $u|_{\partial B} \in H^{s+\frac{1}{2}}(\partial B)$ if $g \in H^{s-\frac{1}{2}}(\partial B)$.

At this point we need to compute the symbol of the Dirichlet-to-Neuman operator and to this end we use the results from [12]. Consider a tubular neighborhood of the boundary ∂B and denote by (x', x_3) the local coordinates in this neighborhood (which in [12, p. 1101] are referred to as the boundary normal coordinates), where x' denotes the local coordinates for the manifold ∂B in a neighborhood of points on ∂B, and $x_3 \in [0, \epsilon)$ is the coordinate in the inward normal direction to ∂B. We have that in the tubular neighborhood $\partial B \times (0, \epsilon)$, $-\Delta - k^2 n$ can be written as

$$D_{x_3}^2 + 2H\frac{1}{i}D_{x_3} + \Delta_{\partial B} - k^2 n,$$

where $\Delta_{\partial B}$ is the Laplace–Beltrami operator on the manifold ∂B, which we assume to have the Riemannian metric (g_{ij}), and H is the mean curvature. Recall $D_j = \frac{1}{i}\partial_j$. From [12] we have that $\partial_{x_3}^2 + \Delta_\Gamma - 2H(x)\partial_{x_3}$ is a local realization of Δ in this tubular neighborhood of ∂B. Exactly in the same way as in [12, section 1], it can be shown that the Dirichle-to-Neumann operator for our problem is a pseudodifferential operator of order one (modulo a smoothing operator). Modifying slightly the calculations in [12] (to account for the lower order term $k^2 n u$ which contributes only to the zero order terms in the symbol) we obtain that

$$D_{x_3} = i\,\mathrm{op}(q_1) + iK + P,$$

where $q_1 \in \mathcal{S}^1(\partial B)$ (symbol of order one), $K \in \mathrm{op}\,\mathcal{S}^0(\partial B)$ (operator with symbol of order zero), and P is a smoothing operator. We refer the reader to Appendix A for the notation concerning symbols. Furthermore, q_1 can be chosen to be real valued and to assume the form

$$q_1 = \sqrt{g^{ij}\xi_i'\xi_j'} \quad \text{for} \quad |\xi'| \geq 1,$$

where we use the Einstein summation for $g^{ij}\xi_i'\xi_j'$ and (g^{ij}) is the inverse of (g_{ij}).

Since D_{x_3} corresponds to the inward normal derivative, $\frac{\partial u}{\partial \nu} - zu = g$ yields

$$-D_{x_3}u - z\frac{1}{i}u = \frac{1}{i}g \quad \text{on} \quad \partial B$$

which gives

$$(\mathrm{op}(q_1) - z)\,u = g - Ku + iPu \quad \text{on} \quad \partial B,$$

where $\mathrm{op}(q_1)$ denotes the pseudodifferential operator with the symbol q_1.

Next, let $\theta \in [-\pi, \pi)$ with $|\theta|$ sufficiently small and define

$$\begin{aligned} \Lambda &:= \{z : \arg z \notin (-\theta, \theta)\}, \\ \Lambda_{R_0} &:= \Lambda \cap \{z : |z| > R_0\}. \end{aligned}$$

Since $q_1 \geq 0$, this choice of z implies that the operator $\mathrm{op}(q_1) - z$ is a hypoelliptic operator with parameter $z \in \Lambda$ of class $\mathrm{op}_z \mathcal{HS}_1^1(\partial B, \Lambda)$, i.e., its symbol satisfies (A.3) in Appendix A. Lemma A.1 in Appendix A gives that for $z \in \Lambda_{R_0}$ with sufficiently large R_0

$$\| \left(\mathrm{op}(q_1) - z\right)^{-1} \|_{H^{s-\frac{1}{2}}(\partial B) \to H^{s-\frac{1}{2}}(\partial B)} \leq C|z|^{-1} \tag{4.6}$$

and

$$\| \left(\mathrm{op}(q_1) - z\right)^{-1} \|_{H^{s-\frac{1}{2}}(\partial B) \to H^{s+\frac{1}{2}}(\partial B)} \leq C \tag{4.7}$$

for some positive constant $C > 0$. Furthermore estimate (A.2) in Appendix A gives that

$$\|Ku\|_{H^{s-\frac{1}{2}}(\partial B)} \leq C\|u\|_{H^{s-\frac{1}{2}}(\partial B)}$$

with a similar estimate for the C^∞ part Pu. Combining the latter estimate with (4.6) yields

$$\|u\|_{H^{s-\frac{1}{2}}(\partial B)} \leq C\left(|z|^{-1}\|g\|_{H^{s-\frac{1}{2}}(\partial B)} + |z|^{-1}\|u\|_{H^{s-\frac{1}{2}}(\partial B)}\right)$$

with some positive constant $C > 0$. Note that from the above we already know that $u \in H^{s-\frac{1}{2}}(\partial B)$ for $s > 0$. Thus choosing z such that $|z| \geq R_0$ for R_0 sufficiently large gives

$$\|u\|_{H^{s-\frac{1}{2}}(\partial B)} \leq C|z|^{-1}\|g\|_{H^{s-\frac{1}{2}}(\partial B)}.$$

In a similar way using (4.7) gives

$$\|u\|_{H^{s+\frac{1}{2}}(\partial B)} \leq C\|g\|_{H^{s-\frac{1}{2}}(\partial B)}.$$

This proves the lemma. ∎

With the help of Lemma 4.1 we can now show that the inverse of B_z exists for $z \in \mathbb{C}$ with modulus sufficiently large.

LEMMA 4.2. *Assume $n(x) = n_1(x) + i\frac{n_2(x)}{k}$, where $n_1(x) > 0$ and $n_2(x) \geq 0$ (non-identically zero) for $x \in B$. Then there exists $z \in \mathbb{C}$ with sufficiently large $|z|$ such that B_z has a bounded inverse $R_z : H^{-\frac{1}{2}}(\partial B) \to H^{\frac{1}{2}}(\partial B)$.*

Proof. Choose z that satisfies the assumptions in Lemma 4.1, i.e., $\arg z \neq 0$ and $\arg z$ is fixed. Let $g = B_z\alpha$, where $\alpha \in H^{\frac{1}{2}}(\partial B)$. From Lemma 4.1

$$\|\alpha\|_{H^{\frac{1}{2}}(\partial B)} \leq C\|g\|_{H^{-\frac{1}{2}}(\partial B)}$$

for some constant $C > 0$. Consequently B_z is injective and has closed range. We now prove that B_z has dense range in $H^{-\frac{1}{2}}(\partial B)$. To this end, let $h \in H^{\frac{1}{2}}(\partial B)$ be such that

$$\langle B_z\alpha, h\rangle = 0 \quad \forall \alpha \in H^{\frac{1}{2}}(\partial B).$$

We want to show that $h = 0$, which proves that B_z has dense range. Here $\langle \cdot, \cdot \rangle$ denotes $H^{-\frac{1}{2}}$, $H^{\frac{1}{2}}$ duality. Let $w \in H^1(D)$ be the unique solution of

$$\begin{aligned} \Delta w + (k^2 n_1 - ikn_2)w &= 0 \quad \text{in} \quad B, \\ w &= h \quad \text{on} \quad \partial B. \end{aligned}$$

Then

$$\left\langle \frac{\partial u}{\partial \nu}, h \right\rangle = \int_{\partial B} \frac{\partial u}{\partial \nu} \overline{w} ds = \int_B \Delta u \overline{w} dx + \int_B \nabla u \nabla \overline{w} dx$$
$$= -\int_B (k^2 n_1 + ikn_2) u \overline{w} dx + \int_B \nabla u \nabla \overline{w} dx$$
$$= \int_B u \Delta \overline{w} dx + \int_B \nabla \overline{w} \nabla u dx = \int_{\partial B} \frac{\partial \overline{w}}{\partial \nu} \alpha ds.$$

Since

$$\left\langle \frac{\partial u}{\partial \nu}, h \right\rangle - \langle z\alpha, h \rangle = \langle B_z \alpha, h \rangle = 0,$$

then

$$\int_{\partial B} \left(\frac{\partial \overline{w}}{\partial \nu} - z\overline{w} \right) \alpha ds = 0.$$

Noting that $\alpha \in H^{\frac{1}{2}}(\partial B)$ is arbitrary, this implies that

$$\frac{\partial \overline{w}}{\partial \nu} - z\overline{w} = 0,$$

and hence

$$B_z \overline{h} = 0.$$

Applying Lemma 4.1 again, we obtain that $h = 0$. Since B_z is injective and has closed dense range in $H^{-\frac{1}{2}}(\partial B)$, this proves that B_z has a bounded inverse. ∎

Remark 1. Lemmas 4.1 and 4.2 show that for $z \in \mathbb{C}$ with $|z|$ large enough and $\arg z \neq 0$, the resolvent R_z is well defined and is bounded from $H^{s-\frac{1}{2}}(\partial B)$ to $H^{s+\frac{1}{2}}(\partial B)$ for all $s \geq 0$, i.e., it is a smoothing operator of order one.

4.1. Spectral results on the Stekloff eigenvalue problem. Here we prove the existence of Stekloff eigenvalues and the completeness of the associated eigenvectors. To this end, we fix a $z \in \mathbb{C}$ with $|z|$ large enough and $\arg z \neq 0$ and consider the bounded linear operator $R_z : H^1(\partial B) \to H^1(\partial B)$ which is well defined due to Lemma 4.2 and Remark 1. We apply the Agmon theory on the spectrum of Hilbert–Schmidt operators (see [2]).

LEMMA 4.3. *Let $p > (m-1)/2$, $m = 2, 3$, denote an integer. Then $R_z^p : H^1(\partial B) \to H^1(\partial B)$ is a Hilbert–Schmidt operator.*

Proof. The proof follows exactly the lines of the proof of [2, Theorem 13.5] or in [13, Lemma 4.1]. The main ingredient is the Sobolev embedding theorem applied to our C^∞ compact $(m-1)$-dimensional manifold ∂B, $m = 2, 3$. More precisely, for $p > (m-1)/2$ we have that $H^p(\partial B) \subset L^\infty(\partial B)$ and the following inequalities hold for $u \in H^p(\partial B)$:

$$|u(x)| \leq \gamma \|u\|_{H^p(\partial B)}^{(m-1)/2p} \|u\|_{L^2(\partial B)}^{1-(m-1)/2p}$$

and

$$\left| \frac{\partial u}{\partial \nu}(x) \right| \leq \gamma \|u\|_{H^{p+1}(\partial B)}^{(m-1)/2p} \|u\|_{H^1(\partial B)}^{1-(m-1)/2p},$$

where $x \in \partial B$ and $\gamma > 0$ depends only on ∂B and p. To prove this, since ∂B is a

compact manifold it can be covered by a finite number of charts $(\Gamma_\ell, \phi_\ell)_{\ell=1,\dots,L}$ such that for any ℓ in (Γ_ℓ, ϕ_ℓ) the Riemannian metric (g_{ij}) is bounded above and below by the Eucledian metric, i.e., $(1/2)\delta_{ij} \leq g_{ij} \leq 2\delta_{ij}$. Then by standard arguments using a partition of unity (see, e.g., [11]) one can use the Sobolev embedding theorem (see, e.g., [1, Theorem 4.12]), and the estimate in [2, Lemma 13.2] for open bounded regions in $\mathbb{R}^{m-1}$, to derive the above inequalities. The result of the lemma now follows from [2, Theorem 13.5] (see also the proof in [13, Lemma 4.1]) since $R_z^p : H^1(\partial B) \to H^{1+p}(\partial B)$ for $p > (m-1)/2$. ∎

Remark 2. Note that in the case when $B \subset \mathbb{R}^2$, the above proof shows that R_z is a Hilbert–Schmidt operator, which can also be directly proven using a parametrization of the curve and an eigenfunction expansion.

We have now all the ingredients to arrive at the final spectral theorem. To this end we apply the following theoretical result that is a direct consequence of combining [13, Proposition 4.2] and the proof of [13, Theorem 5]. Indeed the statement here is a slight modification of the celebrated result of Agmon stated in [2, Theorem 16.4] (see [2] for the definition of generalized eigenfunctions).

THEOREM 4.4. *Let H be a Hilbert space and $S : H \to H$ be a bounded linear operator. If λ^{-1} is in the resolvent of S, define*

$$S_\lambda = S(I - \lambda S)^{-1}. \tag{4.8}$$

Assume $S^p : H \to H$ is a Hilbert–Schmidt operator for some integer $p \geq 2$. For the operator S, assume there exist N rays with bounded growth where the angle between any two adjacent rays is less that $\frac{\pi}{2p}$. More precisely assume there exist $0 \leq \theta_1 < \theta_2 < \cdots < \theta_N < 2\pi$ such that $\theta_k - \theta_{k-1} < \frac{\pi}{2p}$ for $k = 2, \dots, N$ and $2\pi - \theta_N + \theta_1 < \frac{\pi}{2p}$ satisfying the condition that there exists $r_0 > 0$, $c > 0$ such that $sup_{r \geq r_0} \|(S)_{re^{i\theta_k}}\|_{H \to H} \leq c$ for $k = 1, \dots, N$. Then eigenvalues of S exist and the space spanned by the generalized eigenfunctions corresponding to nonzero eigenvalues is dense in the closure of the range of S^p.

A consequence of this result is the following theorem.

THEOREM 4.5. *Assume $n(x) = n_1(x) + i\frac{n_2(x)}{k}$, where $n_1 > 0$ and $n_2 \geq 0$ (non-identically zero). Then there are infinitely many eigenvalues of R_z and the associated generalized eigenfunctions are dense in $H^1(\partial B)$.*

Proof. For both $\mathbb{R}^2$ and $\mathbb{R}^3$ it suffices to apply Theorem 4.4 with $S = R_z$ and $p = 2$. Note that in $\mathbb{R}^2$ since R_z is Hilbert–Schmidt it is also possible to use a slightly different version of this theorem for $p = 1$ (see [13]). Lemmas 4.1 and 4.2 guarantee that we can find directions θ_j as required in Theorem 4.4 for which the bounded growth condition is satisfied. Note that $(R_z)_\lambda = R_{z+\lambda}$, where $(R_z)_\lambda$ is defined by (4.8) with S replaced by R_z. Hence, it only remains to prove that the closure of the range of R_z^2 is dense in $H^1(\partial B)$. By a density argument, it suffices to show the range of R_z is dense in $H^1(\partial B)$. Indeed for any $\alpha \in H^1(\partial B)$, let $g = B_z\alpha$ be in $L^2(\partial B)$. Let $g_\ell \in H^1(\partial B)$ be such that

$$g_\ell \to g \quad \text{in} \quad L^2(\partial B) \ \text{ as } \ell \to +\infty.$$

Then

$$R_z g_\ell \to R_z g = \alpha \quad \text{in} \quad H^1(\partial B)$$

since $R_z : L^2(\partial B) \to H^1(\partial B)$ is bounded, which proves that R_z has dense range in $H^1(\partial B)$. Hence the theorem is proven. ∎

We can now state the spectral properties of the Stekloff eigenvalue problem including here the case of $n_2 \equiv 0$ discussed in section 2. Note that if z is such that R_z is well defined and letting $\mathcal{T}$ denote the set of Stekloff eigenvalues, then $\{\mu = (\lambda - z)^{-1},\ \lambda \in -\mathcal{T}\}$ is the set of the eigenvalues of R_z.

THEOREM 4.6. *Assume* $n(x) = n_1(x) + i\frac{n_2(x)}{k}$, *where* $n_1 > 0$ *and* $n_2 \geq 0$. *There exist infinitely many Stekloff eigenvalues in the complex plane and they form a discrete set without finite accumulation points. The associated generalized eigenvectors are dense in* $H^1(\partial B)$.

We end this section with a result on the location of Stekloff eigenvalues in the complex plane which is a byproduct of the proof of Lemmas 4.1 and 4.2.

THEOREM 4.7. *For arbitrary* $\epsilon > 0$, *all Stekloff eigenvalues except for finitely many lie in the* ϵ*-wedge*

$$\mathcal{S} := \{z \in \mathbb{C} : \pi - \epsilon \leq \arg(z) \leq \pi\},$$

where we define $0 \leq \arg(z) < 2\pi$.

Proof. Consider the ball B_R of radius R for $R := R_\epsilon$ large enough. From the proof of Lemma 4.2 there are no eigenvalues outside $B_R \cup \mathcal{S}$. Since there are no interior accumulation points of the eigenvalues, there are only at most finitely many eigenvalues in $\overline{B_R} \cap \mathcal{S}$. We have already proved the positivity of the imaginary part of the eigenvalue after (4.1). ∎

Example 3. As in section 2, by separation of variables, one can see that Stekloff eigenvalues for the unit ball in $\mathbb{R}^3$ and refractive index $n = n_1 + i\frac{n_2}{k}$ are

$$\lambda_m = -k\sqrt{n}\frac{j_m'(k\sqrt{n})}{j_m(k\sqrt{n})},$$

where j_m denotes a spherical Bessel function of order m. For large m we have that (see [9])

$$j_m(t) \approx t^m/(2m+1)!!,$$
$$j_m'(t) \approx mt^{m-1}/(2m+1)!!,$$

which imples that

$$\lambda_m \approx -\frac{k\sqrt{n}m}{k\sqrt{n}} = -m.$$

Hence in this case the (complex) Stekloff eigenvalues tend to the negative real axis.

5. Numerical examples. We now show some numerical results that support the claims in the paper where, for the sake of simplicity, we restrict our attention to examples in $\mathbb{R}^2$ instead of $\mathbb{R}^3$. We will show results for three background regions D: (1) the unit disk as discussed earlier in the paper, (2) the square with sides of length $\sqrt{2}$, and (3) an L-shaped domain formed by removing the square $[0.1, 1.1] \times [-1.1, -0.1]$ from the square $[-0.9, 1.1] \times [-1.1, 0.9]$ (see Figure 4). Except for section 5.3, we always use $B = D$.

5.1. Changes in eigenvalues due to flaws. We start by investigating the sensitivity of Stekloff eigenvalues to the size and position of flaws by using a finite element method to find approximations of the lowest Stekloff eigenvalues. For the circular domain we can also compute the Stekloff eigenvalues exactly via (2.6) so this case is useful to confirm the accuracy of the inverse algorithm.

Our Stekloff eigensolver is based on approximating the operator T defined in (2.3). Let V_h denote the space of continuous piecewise cubic finite elements on a mesh $\mathcal{T}_h$ of B consisting of regular triangles of maximum diameter $h > 0$. The computational domain is then $B_h = \cup_{K \in \mathcal{T}_h} K$. Let S_h denote the space of traces of functions in V_h to ∂B_h (these are just continuous piecewise cubic finite elements on the mesh on ∂B_h induced by the volume mesh). Given $\mu \in L^2(\partial B)$, we can define the discrete analogue of v_μ denoted $v_{\mu,h} \in V_h$ as the unique solution of

$$(\nabla v_{\mu,h}, \nabla \xi) - k^2 (n v_{\mu,h}, \xi) = \langle \mu, \xi \rangle \quad \forall \xi \in V_h. \tag{5.1}$$

Since we have assumed that k^2 is not a Neumann eigenvalue for the Laplacian on B we can be sure that if h is small enough this problem has a unique solution. Then we define $T_h : S_h \to S_h$ by

$$T_h \mu = v_{\mu,h}|_{\partial B}.$$

We then see that λ_h is a discrete Stekloff eigenvalue with eigenfunction $\mu_h \in S_h$ if $\mu_h \neq 0$ and

$$-\lambda_h T_h \mu_h = \mu_h$$

which is a direct analogue of (2.4). A matrix representing T_h can be computed by solving the source problem (5.1) for each nodal basis function in S_h. The eigenvalues can then be computed using the MATLAB `eig` command.

Note that for the disk $\partial B_h \neq \partial B$, but for the square and L-shaped domain the computational domain coincides with the true domain. For the disk we still see convergence of the computed eigenvalues to the exact eigenvalues as the mesh is refined.

An alternative to this approach is to use (2.1) directly. This will result in a large sparse eigenvalue problem. Both approaches give good approximations to the eigenvalues of the disk (compared to analytic solutions) and to eigenvalues computed using a very slight modification of the "Eigenvalues" code from http://pages.uoregon.edu/siudeja/software.php which computes Stekloff eigenvalues for the Laplace equation in 2 and 3 dimensions using the direct approach mentioned in this paragraph [10]. We have found that using T_h is convenient since only approximate Stekloff eigenvalues are computed.

For each domain we use $k = 1$ (which give a wavelength of 2π) and choose $n(x) = 4$. The "flaw" is a disk $C \subset B$ disjoint from ∂B centered at the point (x_c, y_c) and of radius r_c (obviously more physically relevant flaws such as cracks need to be considered for specific applications—the disk is just a simple example). Then for the flawed domain we have that

$$n(x) = \begin{cases} 1 & \text{for } x \in C, \\ 4 & \text{otherwise.} \end{cases}$$

For each of the example scatterers, we compute eigenvalues λ_j, $j = 1, \ldots,$ for the background and $\lambda_{c,j}(x_c, y_c, r_c)$, $j = 1, \ldots,$ for the flawed medium (ordered by value). Because we can only determine the first few eigenvalues from the far field data we limit ourselves to considering λ_j, $1 \leq j \leq 7$. Then, in Figure 3, we plot the relative change defined as

$$\frac{\lambda_{c,j^*}(x_c, y_c, r_c) - \lambda_j}{|\lambda_j|}, \quad j = 1, \ldots, 7, \tag{5.2}$$

where j^* is the index that minimizes the magnitude of the above ratio. We use this

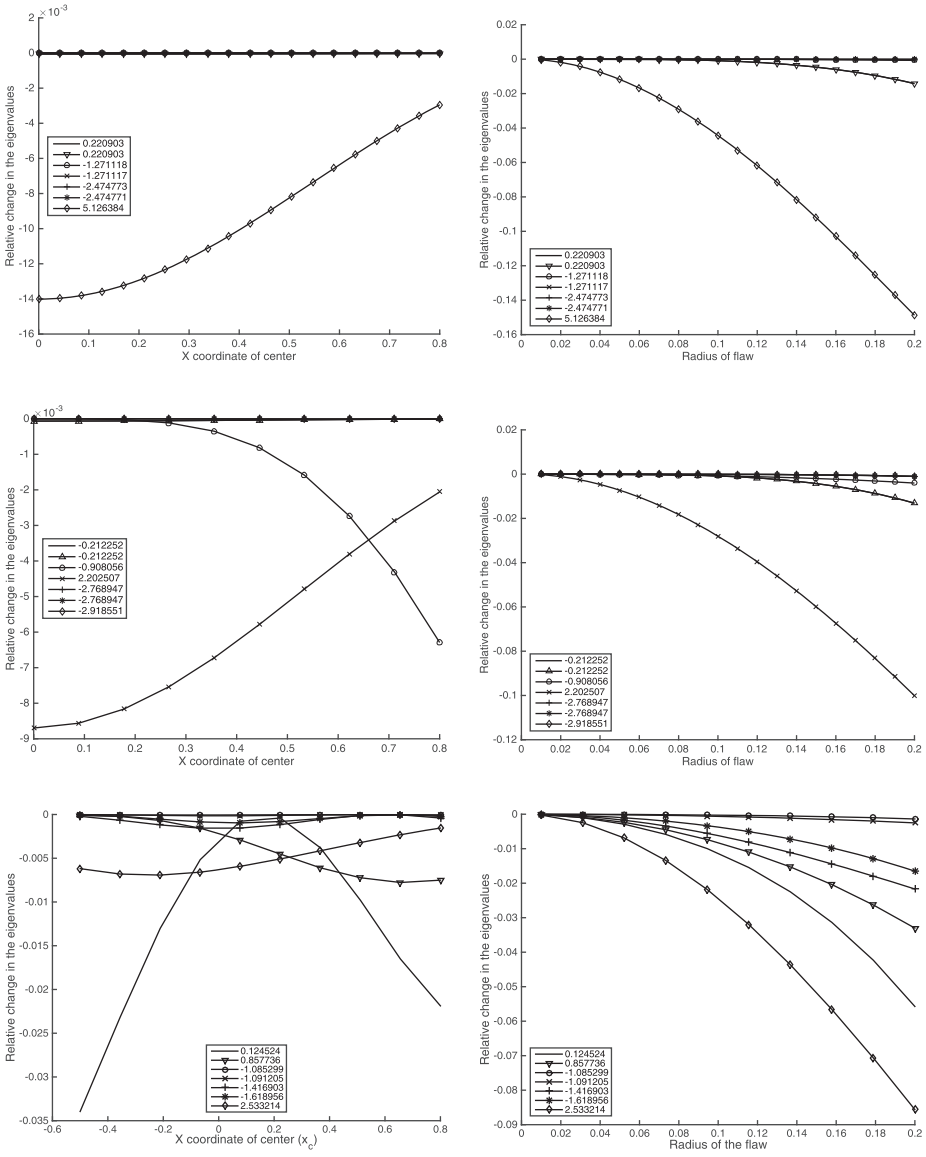

FIG. 3. *Sensitivity of Stekloff eigenvalues to changes in position and size of flaws (see the text for the definition of the flaw in each case). We plot the relative change in the first seven Stekloff eigenvalues for each background shape due to the presence of the flaw (see* (5.2)*). The numbers in the legends refer to the computed eigenvalue of the background. Left column: changes due to the position of the flaw. Right column: changes due to the size of the flaw. Top row: disk. Second row: square. Bottom row: L-shaped domain.*

slightly complicated definition to make sure that as (x_c, y_c, r_c) changes we always use the eigenvalue of the flawed medium closest to the background eigenvalue.

Figure 3 shows plots of the relative change in the first seven eigenvalues (defined by (5.2)) as a function of position (left column) and size (right column) of the flaw. When examining the sensitivity of the eigenvalues to position, the parameters are as follows: for the disk we choose the position of the flaw to be $y_c = 0$ and $0 \le x_c \le 0.8$ with $r_c = 0.05$. For the square we choose $y_c = 0$ and $0 \le x_c \le 0.8$ with $r_c = 0.05$, and for the L-

shaped domain we choose $y_c = 0.4$ and $-0.4 \leq x_c \leq 0.9$ with $r_c = 0.05$. When examining the sensitivity to the size of the flaw, we consider $0.01 \leq r_c \leq .2$ and, for the disk and square, $(x_c, y_c) = (0, 0.3)$, while for the L-shape $(x_c, y_c) = (0.1, 0.4)$. These positions are essentially arbitrary and correspond to the results in Figure 7 discussed later.

For all the background shapes the sensitivity of the eigenvalues to change in the size of the flaw (right column of Figure 3) are broadly similar. In each case at least one of the eigenvalues shows monotonic change as the size of the flaw increases, and thus could be used to monitor the size of flaws.

Considering Figure 3 (left column) we see that for the disk, the eigenvalue $\lambda_7 = 5.126384$ shows the most change due to the flaw regardless of the position of the flaw. For the square, $\lambda_4 = 2.202507$ plays almost the same role, although if the flaw is close to the corner of the square, $\lambda_3 = -0.908056$ is most sensitive to the presence of the flaw. For the L-shaped domain the eigenfunctions are more complex and the most sensitive eigenvalue to the presence of the flaw varies depending on the position of the flaw.

To understand the sensitivity of the eigenvalues to flaws we can use (2.5) with w chosen to be an eigenfunction for the domain. When the eigenfunction is close to zero in the neighborhood of the flaw, the corresponding eigenvalue will be insensitive to the presence of the flaw. In Figure 4 we provide plots of two eigenfunctions for each background domain. In the top left panel we show the eigenfunction corresponding to $\lambda_7 \approx 2.202507$ for the disk which corresponds to $m = 0$ and $n = 4$ in (2.6). As is to be expected for $k = 1$ the eigenfunction corresponding to $m = 0$ is nonzero throughout the domain (and decaying towards the boundary). Hence λ_7 is sensitive to the presence of the flaw as shown in Figure 3 (top left panel). For the square, we show in the middle row, left panel of Figure 4, the eigenfunction corresponding to $\lambda_7 \approx -2.918551$. This eigenfunction is of small magnitude in the domain $0 < x < 1$ and $y \approx 0$, so the small flaw positioned there causes a small change in the eigenvalue and this eigenvalue is insensitive to the presence of the flaw in this part of the domain. Finally for the L-shaped domain we show, in the bottom row of Figure 4, the eigenfunctions for $\lambda_1 \approx 0.124524$ (left panel) and λ_{14} (right panel). The nodal line of this eigenfunction corresponding to roughly $x = 0.1$ explains the lack of sensitivity of λ_1 to flaws in this region shown in Figure 3 (bottom left panel).

We have observed, as shown in the right column of Figure 4, that eigenfunctions corresponding to larger eigenvalues are typically nonzero in a smaller and smaller neighborhood of the boundary. This evanescent behavior is unsurprising for the disk given that the eigenfunctions are Bessel functions, but we have no explanation for this behavior for the other figures. It suggests that Stekloff eigenvalues of larger magnitude (even if we could measure them from the far field pattern) would only be sensitive to flaws near the surface.

5.2. Detecting Stekloff eigenvalues from far field data. In this section we will demonstrate finding Stekloff eigenvalues from far field data for real $n(x)$. This includes comparing Stekloff eigenvalues for domains with and without flaws. We first compute scattering data (approximating u_∞), then for several choices of the Stekloff parameter λ we approximate the corresponding far field pattern h_∞ using $B = D$ and then solve a discrete analogue of the far field equation (3.6) using Tikhonov regularization with a fixed Tikhonov parameter $\alpha = 10^{-5}$. We performed limited tests using the more usual Morozov procedure [9] but found no advantage and so opted for the simpler approach here.

For the forward problem, we choose a piecewise constant function $n(x)$ and compute the solution of the forward problem using a cubic finite element method truncat-

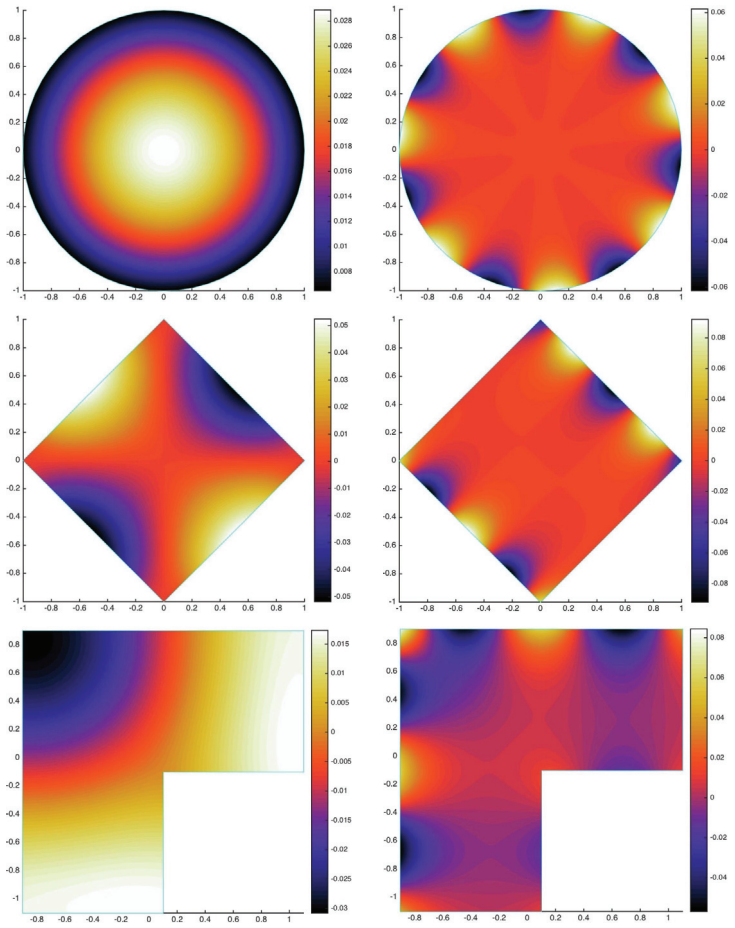

FIG. 4. *Density plots of the eigenfunctions for the three domains in this study. Top row: disk (left: corresponding to λ_7, right corresponding to λ_{14}). Middle row: square (left: corresponding to λ_7, right corresponding to λ_{14}). Bottom row: L-shape domain (left: corresponding to λ_1, right corresponding to λ_{14}).*

ing the mesh by a perfectly matched layer with constant absorption parameters. We choose meshes where the triangle diameter is approximately 1/30 of the wavelength in the element.

In each case we use 51 incoming waves with directions d_j, $j = 1, \ldots, 51$, uniformly on the unit circle and hence compute a 51×51 matrix U with $U_{\ell,m} \approx u_\infty(d_\ell, d_m)$. Similarly we obtain a matrix H approximating h_∞. In some experiments we corrupt the measured data U as follows. We choose $\epsilon > 0$ and set

$$U^\epsilon_{\ell,m} = U_{\ell,m}(1 + \epsilon(\zeta_{l,m} + i\mu_{\ell,m})/\sqrt{2}), \quad 1 \le \ell, m \le 51,$$

where $\zeta_{\ell,m}$ and $\mu_{\ell,m}$ are uniformly distributed random numbers in $[-1, 1]$ computed using the MATLAB `rand` command. Setting the data vector b_z with ℓth entry $b_{z,\ell} = \phi_\infty(d_\ell, z)$, $1 \le \ell \le 51$, for some $z \in B$ we compute an approximation to the Herglotz kernel g using Tikhonov regularization, setting $F^\epsilon = U^\epsilon - H$ and

$$g^\epsilon_z = ((F^\epsilon)^* F^\epsilon + \alpha I)^{-1}(F^\epsilon)^* b_z,$$

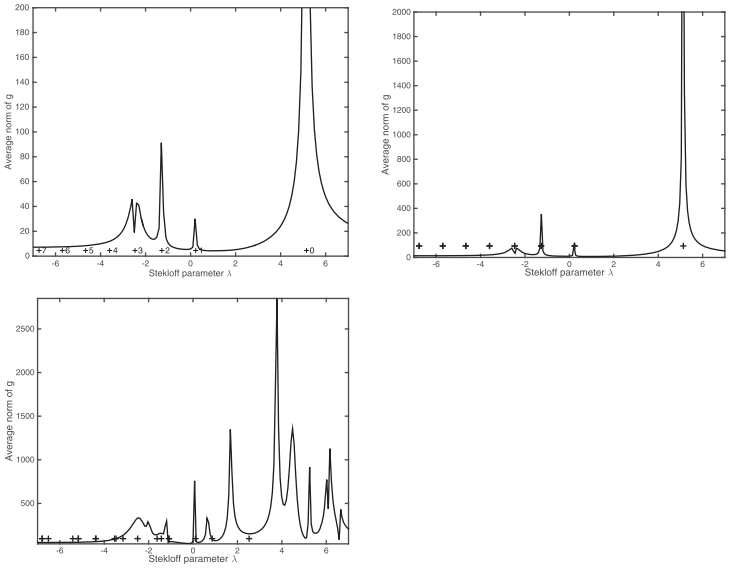

FIG. 5. *Results when $n(x) = 4$ and noise level $\epsilon = 0$. We plot the average of the ℓ^2 norm of g_z^ϵ against the Stekloff parameter λ. The crosses in each figure show the position of Stekloff eigenvalues computed by our finite element eigenvalue code. Top left: disk (integers near the crosses refer to the order of the Bessel function): Top right: square. Bottom left: L-shaped domain.*

where the superscript $*$ denotes the conjugate transpose of the given matrix. This is repeated for 20 randomly placed $z \in B$ and the norm of g_z^ϵ is averaged.

As usual we use the ℓ^2 norm of g^ϵ as surrogate for $\|v_g\|_{L^2(B)}$ and limited testing suggests this approach yields similar results to the use of the more expensive $\|v_g\|_{L^2(B)}$. The choice of 51 directions and 20 points $z \in B$ is essentially arbitrary, but we need sufficiently many incoming waves to enable an approximation of the far field operator.

Our first results in Figure 5 are for $\epsilon = 0$ and $n(x) = 4$ in each scatterer. For the square and disk, peaks in the norm of g_z^ϵ correspond well to eigenvalues. Higher eigenvalues cannot be detected. For the more complex L-shaped scatterer there are spurious peaks in the norm of g_z^ϵ to the right of the Stekloff spectrum, and some peaks appear shifted. We shall return to this observation later in section 5.3.

In Figure 6 we investigate detecting changes in the overall refractive index of the scatterer for the disk. Using $n(x) = 4$ and $n(x) = 4.1$ we can solve the far field equation as above, and determine shifts in Stekloff eigenvalues from shifts in the peaks of the averaged norm of g_z^ϵ. The procedure, at least for this scatterer and eigenvalue, does not appear to be markedly affected by low levels of noise.

We have shown that Stekloff eigenvalues can detect changes in the overall refractive index. Another possible application is to detect flaws in objects under test. So our next results address this problem. For the disk and square background scatterers we use a circular flaw of radius $r_c = 0.05$. For the disk and square these are centered at $(x_c, y_c) = (0.3, 0)$. In Figure 7 we verify that we can detect the expected changes in the Stekloff eigenvalues from far field data with added noise at $\epsilon = 0.01$ (right column of Figure 7) and without added noise (left column of the same figure) for the disk and square background scatterer. Here we concentrate on a single eigenvalue. In the case of the disk (top row of Figure 7) it is the one eigenvalue most affected by the flaw ($\lambda \approx 5.1$) and indeed an obvious shift in the peak of the average norm of g indi-

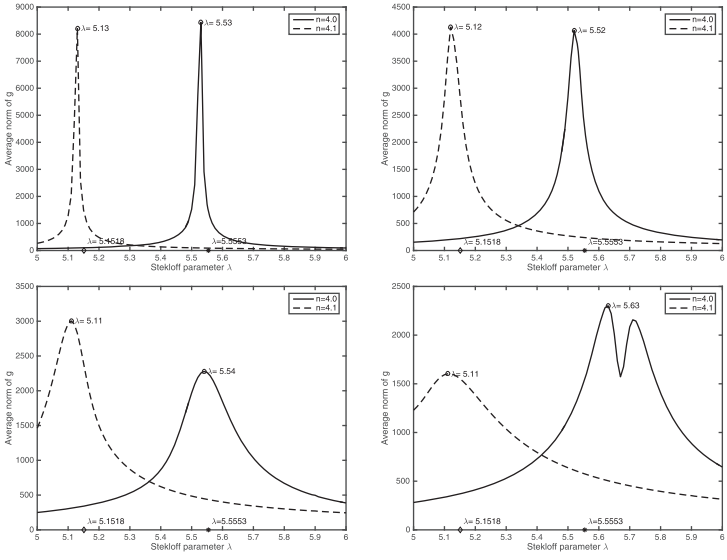

FIG. 6. *Results for detecting changes in the overall refractive index of the disk. The left peak in each figure corresponds to* $n(x) = 4$ *and the right to* $n(x) = 4.1$*. Each figure corresponds to a different noise level* ϵ *and we report the corresponding percentage difference in the* L^2 *norm between the computed far field pattern and the noisy far field pattern: Top left:* $\epsilon = 0$ (0%)*. Top right:* $\epsilon = 0.01$ (0.57%)*. Bottom left:* $\epsilon = 0.05$ (2.9%)*. Bottom right:* $\epsilon = 0.15$ (8.6%)*.*

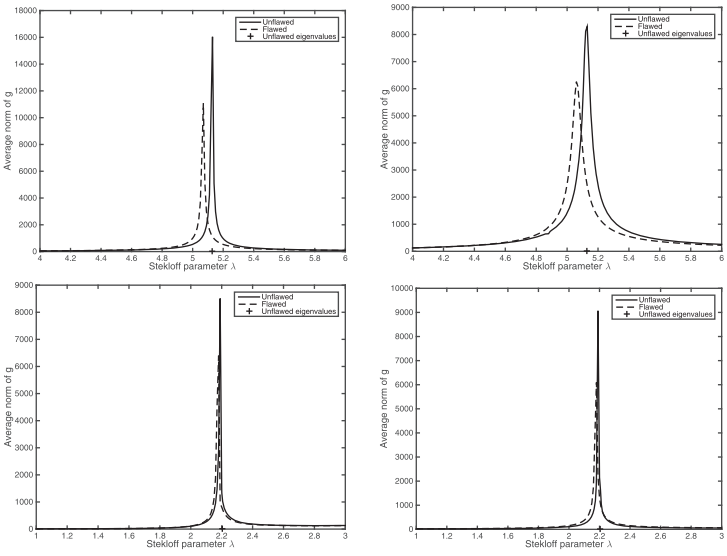

FIG. 7. *Results for detecting flaws in a scatter with background* $n(x) = 4$*. Top row: disk. Bottom row: square. Left column:* $\epsilon = 0$*. Right column:* $\epsilon = 0.01$*.*

cates the change in eigenvalue. The same holds for the square although the change in eigenvalue is smaller as suggested by the results in the middle row of Figure 3. Note that the radius of the flaws in these examples is 0.008 wavelengths.

For the L-shaped domain we choose a range of parameters λ that includes the three Stekloff eigenvalues of smallest magnitude that are visible using far field data in

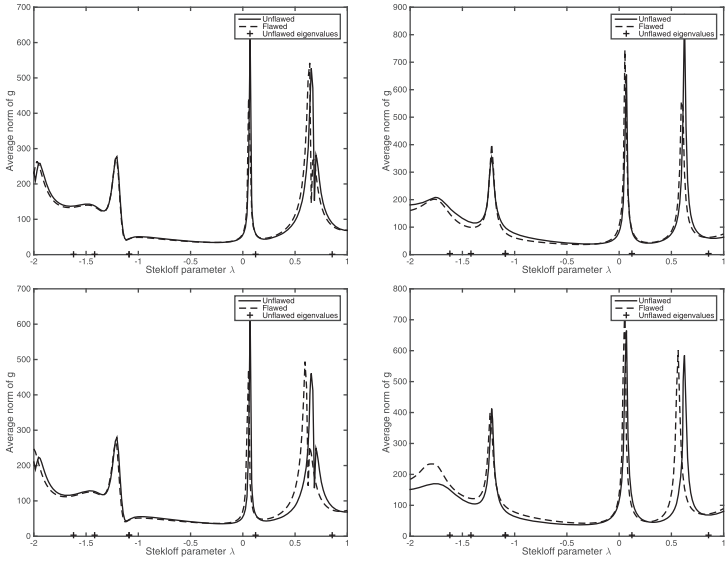

FIG. 8. *Results for detecting flaws in the L-shaped scatterer with background* $n(x) = 4$. *Top row:* $r_c = 0.2$. *Bottom row:* $r_c = 0.3$. *Left column:* $\epsilon = 0$. *Right column:* $\epsilon = 0.01$.

the bottom left panel of Figure 5. We set $(x_c, y_c) = (.1, .4)$, and from Figure 3 (bottom left) we see that this choice of x_c corresponds to a position where the sensitivity of the eigenvalues is low. From Figure 3 (bottom right), we see that detecting the flaw with $r_c = 0.05$ would require a very precise estimate of the eigenvalues, and so in this case we present results for the larger flaw with $r_c = 0.2$ (top row of Figure 8) and $r_c = 0.3$ (bottom row of Figure 8). The shift in observed eigenvalues is as predicted from Figure 3.

5.3. The case $B \neq D$. Our theory allows for B to be a disk centered at the origin containing D in its interior and in this section we perform two preliminary tests of this case. In the first test we use the same unit circle background scatterer, but take B to be a disk of radius 1.5 centered at the origin. In Figure 9 we show detection of Stekloff eigenvalues for fixed $n(x) = 4$ and the shift in the main peak of the averaged norm of g_z^ϵ when changing from $n(x) = 4$ to $n(x) = 4.1$ in the unit disk (the noise level is $\epsilon = 0.01$ for the latter computation). This should be compared to Figure 6 (top right panel). The change in the position (value of λ) for the peak is about $1/2$ that found when $B = D$ so, at least in this case, the choice $B = D$ appears to give more sensitivity to changes in $n(x)$.

We have also tried the case $B \neq D$ when D is the L-shaped domain. In contrast to our theoretical assumption that B is a disk, in our first test we simply used the convex hull of D by adding a triangle to the domain. This did not result in any marked improvement over the case when $B = D$ and is not reproduced here. However, when we chose B to be a disk of radius 1.5 around the scatterer we found that the most of the spurious peaks in the graph of the averaged norm of g (those for λ positive and larger than the largest positive eigenvalue) vanish. This result is shown in Figure 10 (left panel). We also computed the shift in the main peak of the average norm of g_z^ϵ when $n(x)$ changes from 4 to 4.1 in the L-shaped region. The shift is clearly visible (in this case the eigenvalues close to $\lambda = 0$ did not shift appreciably when n is changed).

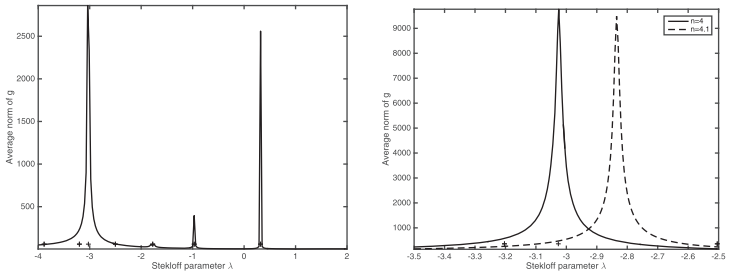

FIG. 9. *Results for detecting Stekloff eigenvalues and changes in the overall refractive index of the unit disk scatterer when $B \neq D$ (in this case B is a disk of radius* 1.5 *centered at the origin). The left panel shows detection of Stekloff eigenvalues when $n(x) = 4$ and should be compared to Figure* 5 *(top left panel). The right panel shows the change in the main peak when $n(x)$ changes from $n(x) = 4$ to $n(x) = 4.1$ and should be compared to Figure* 6 *(top left panel).*

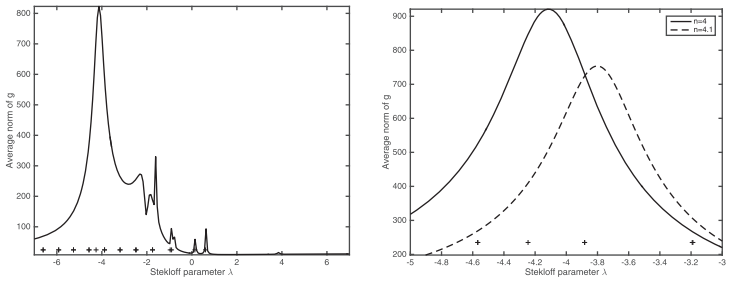

FIG. 10. *Results for detecting Stekloff eigenvalues for the L-shaped domain when B is a disk of radius* 1.5 *(left panel, $n(x) = 4$ and noise $\epsilon = 0$) and detecting changes in the refractive index from $n(x) = 4$ and $n(x) = 4.1$ (right panel, noise $\epsilon = 0.01$). The results in the left panel should be compared to Figure* 5 *(bottom left panel).*

Our explanation for the improvement in this case over setting B to be the convex hull of the vertices of the L-shaped domain is that we are approximating the function u^i (defined in Lemma 3.1) in B by a Herglotz wave function and for a fixed number of incident fields (51 in our case); this can be done better for a disk than for the convex hull of D.

5.4. Complex eigenvalues. First we investigate the sign of the imaginary part of complex Stekloff eigenvalues using our finite element eigensolver. Results are shown in Figure 11. In particular we compare Stekloff eigenvalues for the disk and L-shaped domain for $n(x) = 4$ and $n(x) = 4+4i$. In both cases several eigenvalues have strongly positive imaginary parts.

To demonstrate our claim that Stekloff eigenvalues can be used for absorbing media, we consider the case of the unit disk with $n(x) = 4 + 4i$ with no noise. By choosing the parameter λ on a grid in the complex plane (here a 61×41 rectilinear grid) we can compute the average norm of the Herglotz kernel g for each λ. As proved in section 3, peaks in this grid function should signal complex Stekloff eigenvalues. In Figure 12 we show a contour plot of the base 10 logarithm of the averaged norm of g and also mark the exact Stekloff eigenvalues by asterisks. As we might expect from our study of Stekloff eigenvalues for real $n(x)$, we can detect the first few complex Stekloff eigenvalues quite well.

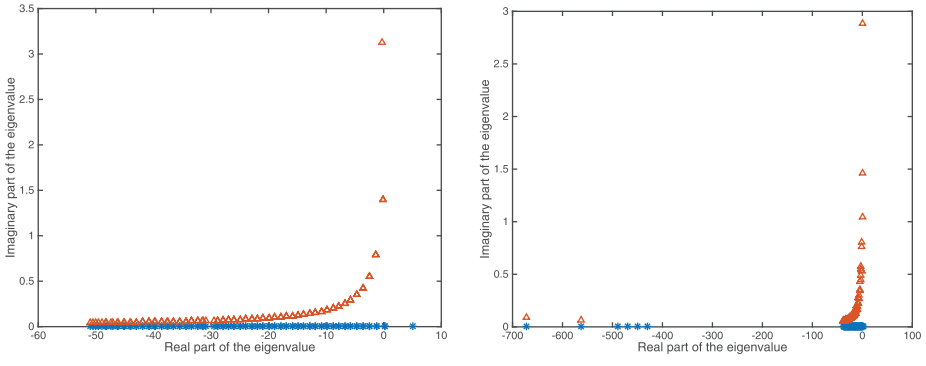

FIG. 11. *Complex eigenvalues corresponding to* $n(x) = 4(1 + i)$ *(marked with red triangles in the complex plane) together with real Stekloff eigenvalues corresponding to* $n(x) = 4$. *Left: disk. Right: L-shape domain.*

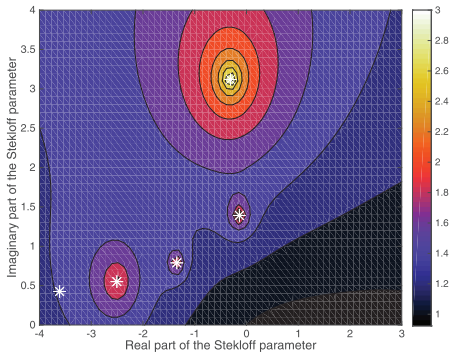

FIG. 12. *A contour plot of the base* 10 *logarithm of the averaged norm of the Herglotz kernel* g *as a function of the real and imaginary parts of the Stekloff parameter* λ. *Exact Stekloff eigenvalues are marked as white* $*$. *The correspondence between peaks in the magnitude of the Herglotz kernel and complex Stekloff eigenvalues is clear.*

6. Conclusion. We have considered the scattering of an incident plane wave by an inhomogeneous medium of compact support with (possibly complex valued) refractive index $n(x)$ such that $n(x)-1$ has support in a bounded region $\overline{D}$. By considering a modified far field operator we have shown that small changes in the refractive index, including flaws in D where $n(x) = 1$, can be detected by using the modified far field operator to determine the changes in Stekloff eigenvalues corresponding to the partial differential equation $\Delta u+k^2n(x)u = 0$ defined in D. A variety of numerical examples have been given showing the effectiveness of this approach for detecting changes in $n(x)$. In particular it has been observed that some Stekloff eigenvalues are more sensitive to changes in $n(x)$ than others and that for domains of complicated geometry it can be advantageous to replace D by a ball containing D in its interior, where $n(x)$ is set equal to one in $B \setminus \overline{D}$. It has also been shown that complex Stekloff eigenvalues corresponding to complex refractive indices can be computed through the use of the same modified far field operator.

Appendix A. Auxiliary results on pseudodifferential calculus. We recall some notions and results on pseudodifferential operators (see, e.g., [3, 14] for details). Here X is a C^∞ manifold, which for our purpose is assumed to be in $\mathbb{R}^m$ and closed.

We say that the C^∞- function $a(x,\xi,\lambda)$ is a symbol with parameter λ in the class $\mathcal{S}_1^\ell(X,\Lambda)$ if it satisfies

$$|\partial_\xi^\alpha \partial_x^\beta a(x,\xi,\lambda)| \le C_{\alpha\beta}(1+|\xi|+|\lambda|)^{\ell-|\alpha|} \tag{A.1}$$

for all $\alpha,\beta \in \mathbb{N}$, $(x,\xi) \in T^*X$, where T^*X is the cotangent bundle of X, and $\lambda \in \Lambda$ where Λ is a closed cone in the complex plane. Moreover, we denote symbols (without parameters) in the class $\mathcal{S}^\ell(X)$ if the above inequality holds for $\lambda = 0$.

Let $\mathrm{op}_\lambda \mathcal{S}_1^\ell(X,\Lambda)$ and $\mathrm{op}\,\mathcal{S}^\ell(X)$ be the spaces of pseudodifferetial operators with symbols in $\mathcal{S}_1^\ell(X,\Lambda)$ and $\mathcal{S}^\ell(X)$, respectively. It is known that for $P \in \mathrm{op}\,\mathcal{S}^\ell(X)$ we have that

$$\|Pu\|_{H^{s-\ell}(X)} \le C\|u\|_{H^s(X)}, \qquad C>0. \tag{A.2}$$

Next we recall the subclass $\mathcal{HS}_1^\ell(X,\Lambda)$ of hypoelliptic symbols with parameters which are those where $a \in \mathcal{S}_1^\ell(X,\Lambda)$ that, in addition, satisfy

$$C_1(|\xi|+|\lambda|)^\ell \le |a(x,\xi,\lambda)| \le C_2(|\xi|+|\lambda|)^\ell \tag{A.3}$$

for $|\xi|+|\lambda| > R$ (see [14, pp. 75–76]). Similarly $\mathrm{op}_\lambda \mathcal{HS}_1^\ell(X,\Lambda)$ denotes the space of pseudodifferential operators with symbol in $\mathcal{HS}_1^\ell(X,\Lambda)$.

The following lemma plays an important role in our spectral analysis of the Stekloff eigenvalue problem and is a particular case of [14, Theorems 9.1 and 9.2].

LEMMA A.1. *Let $A_\lambda \in op_\lambda \mathcal{HS}_1^\ell(X,\Lambda)$. Then, for all $s \ge 0$ there exists $R>0$ such that for $\lambda \in \Lambda_R$ the operator A_λ is invertible with $A_\lambda^{-1} \in op_\lambda \mathcal{HS}_1^{-\ell}(X,\Lambda_R)$, where $\Lambda_R := \Lambda \cap \{\lambda : |\lambda| \ge R\}$. Moreover*

$$\|A_\lambda^{-1}\|_{H^{s-\frac{1}{2}}(X)\to H^{s-\frac{1}{2}}(X)} \le C(1+|\lambda|)^{-\ell}$$

and

$$\|A_\lambda^{-1}\|_{H^{s-\frac{1}{2}}(X)\to H^{s+\frac{1}{2}}(X)} \le C(1+|\lambda|)^{-\ell+1}$$

for some positive constant $C>0$.

Acknowledgment. We thank Professor B.A. Siudeja from the University of Oregon for making his "Eigenvalues" code publicly available.

REFERENCES

[1] R. ADAMS, *Sobolev Spaces*, 3nd ed., Cambridge University Press, Cambridge, 2003.
[2] S. AGMON, *Lectures on Elliptic Boundary Value Problems*, AMS Chelsea Publications, Providence, RI, 2010.
[3] S. ALINHAC AND P. GÉRARD, *Pseudo-differential Operators and the Nash-Moser Theorem*, AMS, Providence, RI, 2007.
[4] F. CAKONI AND D. COLTON, *A Qualitative Approach to Inverse Scattering Theory*, Springer, New York, 2014.
[5] F. CAKONI, D. COLTON, AND H. HADDAR, *On the determination of Dirichlet and transmission eigenvalues from far field data*, C.R. Math. Acad. Sci. Paris, 348 (2010), pp. 379–383.
[6] F. CAKONI, D. COLTON, AND P. MONK, *Transmission Eigenvalues for NDE and Characterization*, Technical report, Task Order 0005, Wright-Patterson Air Force Base, Dayton, OH, 10, 2013.
[7] F. CAKONI AND H. HADDAR, *Special issue on transmission eigenvalues*, Inverse Problems, 29 (2013).
[8] F. CAKONI, I. HARRIS, AND J. SUN, *Transmission eigenvalues and non-destructive testing of anisotropic magnetic materials with voids*, Inverse Problems, 30 (2014), 035016.

[9] D. Colton and R. Kress, *Inverse Acoustic and Electromagnetic Scattering Theory*, 3rd ed., Springer-Verlag, New York, 2013.
[10] A. Girouard, R. S. Laugesen, and B. A. Siudeja, *Steklov eigenvalues and quasiconformal maps of simply connected planar domains*, Arch. Ration. Mech. Anal., 219 (2016), pp. 903–936.
[11] E. Hebey, *Sobolev Spaces on Riemannian Manifolds*, Lecture Notes in Math. 1635, Springer, Berlin, 1996.
[12] J. Lee and G. Uhlmann, *Determining anisotropic real-analytic conductivities by boundary measurements*, Comm. Pure Appl. Math., 42 (1989), pp. 1097–1112.
[13] L. Robbiano, *Spectral analysis of the interior transmission eigenvalue problem*, Inverse Problems, 29 (2013). 104001.
[14] M. A. Shubin, *Pseudodifferential Operators and Spectral Theory*, Springer-Verlag, Berlin, 1987.
[15] J. Wloka, *Partial Differential Equations*, Cambridge University Press, Cambridge, 1987.